Geophysical Journal International

*Geophys. J. Int.* (2022) **231,** 2095–2101
Advance Access publication 2022 August 17
GJI Seismology

https://doi.org/10.1093/gji/ggac315

# A re-examination of ellipticity corrections for seismic phases

Stuart Russell ,[1] John F. Rudge ,[1] Jessica C.E. Irving [2] and Sanne Cottaar [1]

[1] *Bullard Laboratories, Department of Earth Sciences, University of Cambridge, Cambridge, CB3 0EZ, UK. E-mail: sr895@cam.ac.uk*
[2] *School of Earth Sciences, University of Bristol, Bristol, BS8 1RJ, UK*

Accepted 2022 August 9. Received 2022 July 28; in original form 2022 May 13

## SUMMARY

The Earth's ellipticity of figure has an effect on the traveltimes of seismic waves over teleseismic distances. Tables of ellipticity corrections and coefficients have been used by seismologists for several decades; however, due to the increasing variety and complexity of seismic phases in use, current tables of ellipticity coefficients are now outmoded and incomplete. We present a Python package, EllipticiPy, for the calculation of ellipticity corrections, which removes the dependence on pre-calculated coefficients at discrete source depths and epicentral distances. EllipticiPy also facilitates the calculation of ellipticity corrections on other planetary bodies. When applied to both Earth and Mars, the magnitudes of ellipticity corrections are of the order of single seconds and are significant for some seismic studies on Earth but remain negligible on Mars due to other greater sources of uncertainty.

**Key words:** Body Waves; Computational Seismology; Theoretical Seismology; Planetary Seismology.

## 1 INTRODUCTION

It has been known for many decades that the ellipticity of figure of the Earth has a significant effect on the traveltimes of seismic waves propagating over teleseismic distances (e.g. Jeffreys 1935; Bullen 1937). Bullen (1937) tabulated ellipticity corrections for P and S waves for combinations of source colatitude, azimuth and epicentral distance to the receiver. Dziewonski & Gilbert (1976) demonstrated the additional importance of source depth and substantially advanced the mathematics underpinning the calculation of ellipticity corrections by representing the correction as a degree 2 spherical harmonic expansion with calculable coefficients that depend only on phase, source depth and epicentral distance. Dziewonski & Gilbert (1976) also presented tables of these coefficients for commonly used seismic phases in the radially symmetric Parametric Earth Model (PEM; Dziewonski *et al.* 1975).

As the number and complexity of seismic phases in use continued to increase, a re-examination of ellipticity corrections by Kennett & Gudmundsson (1996) advanced the mathematics to allow the calculation of coefficients for diffracted phases. Kennett & Gudmundsson (1996) used the reformulation of Doornbos (1988) coupled with the tau-spline procedure of Buland & Chapman (1983) to produce tabulated coefficients for the most comprehensive list of coefficients yet. Furthermore, Kennett & Gudmundsson (1996) produced a freely available Fortran package (including `ellip` and `ttimel`) to allow seismologists to calculate ellipticity corrections based on interpolating tables of pre-calculated coefficients. Additionally, Kennett & Gudmundsson (1996) demonstrated how coefficients for more complex phases can be calculated by a weighted sum of those for existing phases. In principle, this allowed the calculation of ellipticity corrections for any seismic phase; however, this has the disadvantage of interpolating coefficients calculated at discrete distances and source depths for a single model.

Tables of traveltimes for individual velocity models have long been obsolete in many applications and have been replaced with software that allows the calculation of ray-theoretical traveltimes for a given ray path. One of the foremost software for this is the TauP Toolkit (Crotwell *et al.* 1999) which has since been incorporated into ObsPy (Beyreuther *et al.* 2010), giving maximum utility to the modern seismologist. Nevertheless, interpolating tables is more efficient than ray path integrals and therefore tables are still used where efficiency is the priority, for example when handling large numbers of source–receiver pairs.

In this study, we present a summary of the theory of calculating ellipticity corrections for seismic phases and identify discrepancies in the tabulated coefficients of Kennett & Gudmundsson (1996). Subsequently we present a software package, EllipticiPy, for the calculation of ellipticity corrections that is designed to work alongside ObsPy TauP, allowing the calculation of corrections for any ray path in any velocity model, including of other planets. We then present applications of this package to both Earth and Mars.

## 2 THEORY

Given a planet's ellipticity of figure, $\epsilon(r)$, the relative perturbation of a surface of constant density is

$$r^{-1}\delta r(\vartheta,\phi) = \epsilon(r)\left(1/3 - \cos^2\vartheta\right) = -\frac{2}{3}\epsilon(r)P_2^0(\cos\ \vartheta), \qquad (1)$$

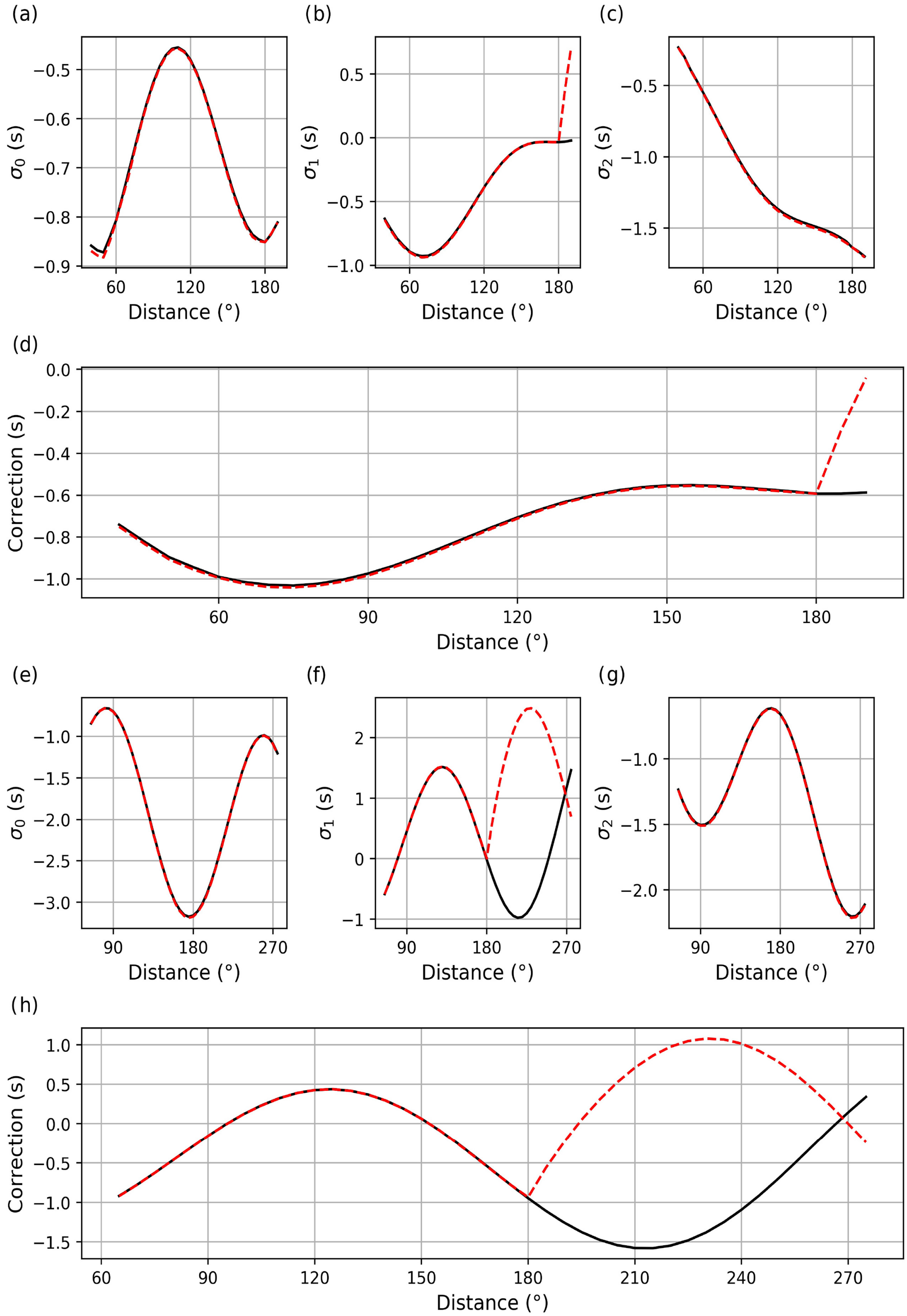


**Figure 1.** Panels (a)–(c) show the values of $\sigma_0$, $\sigma_1$ and $\sigma_2$, respectively, as a function of epicentral distance for a *PP* wave with a source depth of 200 km. The coefficients and corrections of Kennett & Gudmundsson (1996) are shown in dashed red and those from this publication are in solid black. Panel (d) shows the corrections that these coefficients give as a function of epicentral distance for a *PP* wave with a source depth of 200 km, source latitude of 45° and an azimuth of 30°. Panels (e)–(h) show the same but for an $SKKS_{\mathrm{ac}}$ wave with the same source parameters.

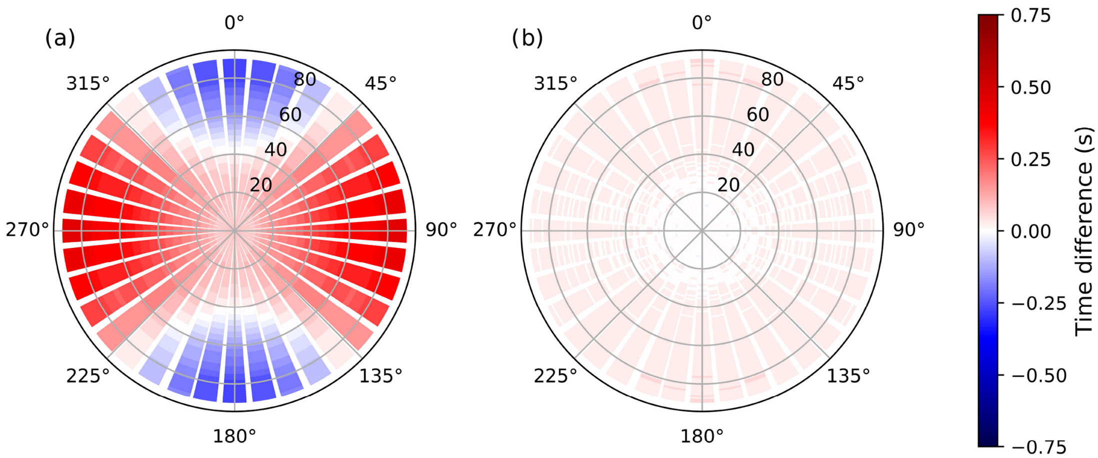


**Figure 2.** Rose diagrams showing the magnitude of the time difference between the elliptical and spherical SPECFEM3D synthetics for (a) uncorrected and (b) corrected *P* waveforms. The angle from the centre point is azimuth from the source and the radius is epicentral distance from the source. The residual once corrected is no more than 0.05 s at all distances and azimuths.

where $r$ is the radius, $\delta r$ is the perturbation from $r$ due to ellipticity, $P_2^0$ is the associated Legendre polynomial of degree 2 and order 0, $\vartheta$ is the co-latitude and $\phi$ is the longitude.

The time correction to be added to a seismic traveltime prediction for a 1-D spherical model to account for the planet's ellipticity of figure can similarly be represented as a degree 2 spherical harmonic (Dziewonski & Gilbert 1976),

$$\delta t = \sum_{m=0}^{2} \sigma_m P_{2,m}(\cos\vartheta_0)\cos m\zeta, \tag{2}$$

where $\vartheta_0$ is the source colatitude, $\zeta$ is the azimuth from source to receiver and $P_{2,m}$ are Schmidt semi-normalized associated Legendre polynomials of degree 2 and order $m$. $\sigma_m$ are calculable coefficients that are dependent only on phase, distance and source depth,

$$\sigma_m = \sum_i \left\{ \int_{q_0}^{q_1} (\xi - 1)\,\epsilon\lambda_m(\theta)\,\mathrm{d}q \right\}_i - \sum_j \left\{ \epsilon\lambda_m(\theta)\,[q]_-^+ \right\}_j$$
$$\mp \sum_k \{\epsilon\lambda_m(\theta) q\}_k \tag{3}$$

where $i$ is a sum over the continuous regions of the ray path and $j$ and $k$ are sums over discontinuities where the ray is transmitted and reflected, respectively. In the sum over $k$, the preceding minus/plus refers to top-side/bottom-side reflections, respectively. $\eta$ and $q$ are ray slowness and vertical slowness, respectively,

$$\eta = \frac{r}{v}, \tag{4}$$

$$q = \sqrt{\eta^2 - p^2}, \tag{5}$$

where $r$ is the radius, $v$ is the velocity and $p$ is the ray parameter, and $\xi$ is a convenient parameter from Bullen (1963):

$$\xi = \frac{\eta}{r}\left(\frac{\mathrm{d}\eta}{\mathrm{d}r}\right)^{-1} = \frac{\mathrm{d}\ln r}{\mathrm{d}\ln\eta}. \tag{6}$$

The sub-scripted vertical slownesses, $q_0$ and $q_1$, are the vertical slownesses at the start and end of the continuous ray segments. $\lambda_m$ is a distance-dependent variable containing a Schmidt semi-normalized associated Legendre polynomial of degree 2 and order $m$

$$\lambda_m(\theta) = -\frac{2}{3} P_{2,m}(\cos\theta). \tag{7}$$

Dziewonski & Gilbert (1976) used an integral over distance in eq. (3); however, this formulation suffers from a discontinuity in distance at the centre of the Earth. Eq. (3) instead uses the formulation of Doornbos (1988), which integrates over vertical slowness without sacrificing the convenience of the original formulation. A full derivation of these equations is given in Supporting Information Section S1.

Ellipticity coefficients for most major phases already exist in published tables (Kennett & Gudmundsson 1996) for the ak135 model (Kennett *et al.* 1995), however some of these coefficients are not correct. Fig. 1 compares the coefficients and corrections for PP and $SKKS_{ac}$ waves from this publication and those of Kennett & Gudmundsson (1996). Below 180° distance there is very good agreement between our study and theirs; however, beyond 180°, they diverge. This divergence is due to a discontinuity in the gradient of $\sigma_1$ in the coefficients of Kennett & Gudmundsson (1996). This discontinuity has a major effect on the value of the ellipticity correction and is incorrect (Kennett, personal communication, 2021). It is only for upgoing $p$ and $s$ waves and at distances greater than 180° for other phases that the $\sigma_1$ coefficient of Kennett & Gudmundsson (1996) is incorrect. It is therefore anticipated that the vast majority of publications will not be affected by these errors as most seismological publications are concerned with minor arc phases and few studies correct upgoing $p$ and $s$.

To benchmark our corrections, SPECFEM3D (Komatitsch & Tromp 2002a,b) synthetics were created in the case of a spherical and an elliptical mesh with a minimum period of approximately 7 s. The time difference between waveforms at the same azimuth and epicentral distance was measured by cross-correlating the windowed waveforms of a particular phase. Fig. 2 shows the measured time differences from uncorrected and corrected synthetic waveforms for a direct *P* wave. Corrections are applied by adding the correction calculated from eq. (2) to the arrival time of the spherical synthetic waveforms. For direct *P* waves, the corrections of this publication are equal to those of Kennett & Gudmundsson (1996). When corrected, the residuals of the corrected waveforms

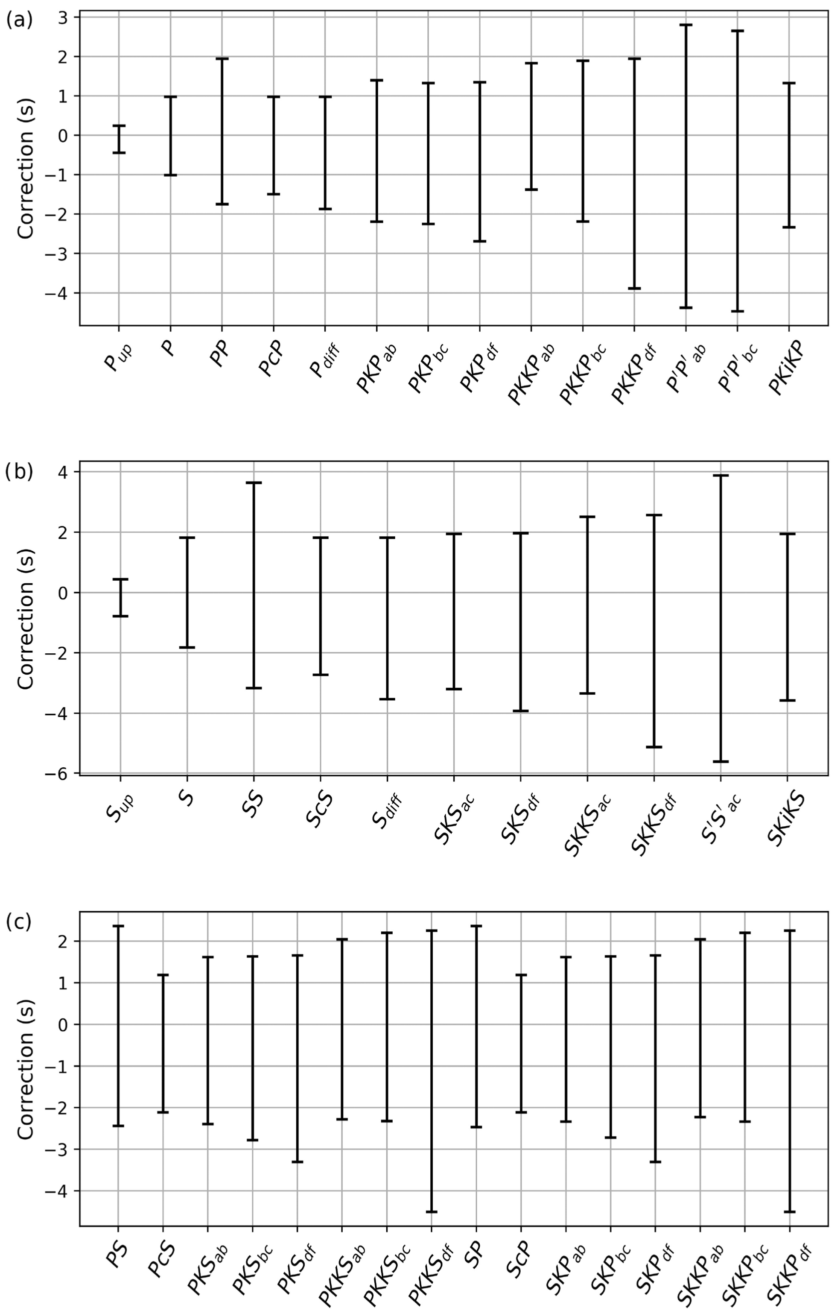


**Figure 3.** Minimum and maximum ellipticity corrections in seconds for commonly used seismic phases. *P* phases are shown in (a), *S* phases in (b) and converted phases in (c). Tabulated values can be found in Supporting Information Section S3. Corrections for depth phases can also be calculated but are not shown here.

are extremely close to zero and have no dependence on azimuth or distance.

## 3 EllipticiPy: A PYTHON PACKAGE FOR THE CALCULATION OF ELLIPTICITY CORRECTIONS

In light of the incorrect coefficients in the existing Fortran software package of Kennett & Gudmundsson (1996), and that the phases used in seismology studies are advancing beyond the scope of current tables, we have created a Python package, EllipticiPy, which calculates an ellipticity correction for a given ray path in any given velocity model by application of the trapezoidal rule to eq. (3). EllipticiPy calculates the values of $\epsilon$ from the density profile in the given 1-D model; a derivation of how $\epsilon$ is calculated can be found in Supporting Information Section S2.

EllipticiPy is designed as a companion to ObsPy TauP that allows the calculation of a spherical traveltime for any ray path in any velocity model. The elliptical traveltime is equal to the sum of the spherical Earth traveltime from ObsPy TauP and the ellipticity correction from EllipticiPy. While EllipticiPy is designed to be used alongside ObsPy, in certain applications where large numbers of source–receiver pairs are used, interpolating tables of pre-calculated coefficients may be more efficient and as such, a function to produce tables of coefficients for specified phases is available in the

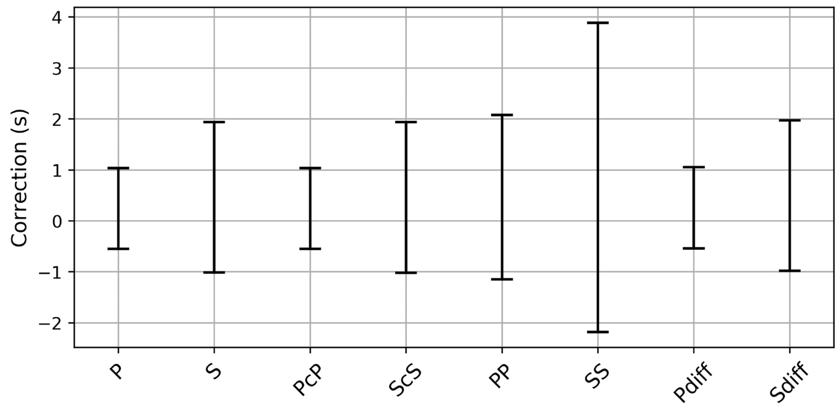


**Figure 4.** Minimum and maximum ellipticity corrections in seconds for phases potentially detectable on Mars at the InSight Lander location (4.50°N, 135.62°E).

**Table 1.** Spherical arrival times, ellipticity corrections and elliptical arrival times for seismic phases potentially detectable at the InSight Lander (4.50°N, 135.62°E) from a hypothetical event in Cerberus Fossae (11.28°N, 166.37°E).

| Phase | Spherical arrival time (s) | Correction (s) | Elliptical arrival time (s) |
|---|---|---|---|
| *P* | 242.13 | 0.39 | 242.52 |
| *PP* | 259.19 | 0.42 | 259.61 |
| *PcP* | 401.87 | 0.71 | 402.57 |
| *S* | 429.46 | 0.68 | 430.14 |
| *SS* | 456.63 | 0.74 | 457.37 |
| *ScS* | 740.85 | 1.30 | 742.15 |

package. Moreover, tables of coefficients in the exact same form as Kennett & Gudmundsson (1996) have been computed (see Supporting Information Section S4). Another package based on dynamic ray tracing, `raydyntrace` (Tian *et al.* 2007), can, amongst other routines, calculate ellipticity corrections; however, it is not as versatile for that specific purpose as EllipticiPy. The use of ObsPy TauP within EllipticiPy enables complex phases to be handled easily, including diffracted phases, and EllipticiPy can be applied to other planets.

In recent decades, seismology has been applied to other bodies in the solar system and, similar to ObsPy TauP, EllipticiPy can also be applied to velocity models of other planets. Seismic waves have now been used to study the internal structure of the Moon (e.g. Latham *et al.* 1973; Garcia *et al.* 2019) and more recently Mars (e.g. Khan *et al.* 2021; Knapmeyer-Endrun *et al.* 2021; Stähler *et al.* 2021). These bodies have a different ellipticity of figure to the Earth which EllipticiPy calculates in the same way as for the Earth (see Supporting Information Section S2). As extra-terrestrial seismology advances it is likely that elliptical effects will need to be considered in the future. It should be noted that the Darwin–Radau equation (Bullen 1975) must hold true in order for the accurate calculation of $\epsilon$, requiring that the body is in hydrostatic equilibrium and is an ellipsoid of revolution.

## 4 APPLICATIONS

### 4.1 Ellipticity corrections on the Earth

Ellipticity corrections on the Earth are of the order of single seconds. Fig. 3 presents the minimum and maximum ellipticity corrections for common seismic phases. These can be found in tabular format in Supporting Information Section S3. These corrections have been calculated by a systematic search over source depths from 0 to 700 km, source latitudes from −90° to 90°, azimuths from 0° to 360° and all integer distances for which that phase has a ray theoretical arrival predicted by ObsPy TauP in PREM (Dziewonski & Anderson 1981). These values therefore represent the full range of potential ellipticity corrections for these phases in PREM but true ranges might be different for realistic source–receiver geometries in a specific application.

Ellipticity corrections are generally larger for *S* waves than *P* waves due to their lower velocities. For longer period body-wave studies these corrections will be small relative to the wavelength of the signal, but for some studies these corrections are non-negligible compared to the magnitude of time anomalies that are interpreted. For high–frequency studies, ellipticity corrections should be routinely applied when interpreting absolute arrival times. This is especially true for more complex phases with long ray paths that have generally larger corrections.

For studies that use differential times, ellipticity corrections are likely to be less significant provided the phases have similar paths through the Earth. For *SmKS* differential times (e.g. Tanaka 2007; Wu & Irving 2020), the differential ellipticity corrections are of the order of hundreds to a couple of tenths of a second and are of minimal significance. However, for phases with vastly different ray paths, for example *P4KP–PcP* differential time studies (e.g. Tanaka 2010), the differential ellipticity corrections are up to two seconds and non-negligible.

### 4.2 Ellipticity corrections on Mars

We have implemented a velocity model of Mars (model InSight_KKS_GP from Khan *et al.* 2021; Knapmeyer-Endrun *et al.* 2021; Stähler *et al.* 2021) in EllipticiPy in order to assess the effect of ellipticity of the Mars on seismic waves. The Mars is approximately twice as elliptical than the Earth at the surface (Bills & Ferrari 1978) but its radius is approximately half that of the Earth. Furthermore, the core fraction by radius is approximately similar to that of the Earth (Stähler *et al.* 2021). The result of this combination is that ellipticity corrections for the Mars have a similar magnitude to those for the Earth but the traveltimes on the Mars are smaller.

Fig. 4 shows the minimum and maximum corrections for seismic phases that either have been detected on the Mars or could potentially be detected on the Mars: *P*, *PP*, *S*, *SS* (Khan *et al.* 2021) and *ScS* (Stähler *et al.* 2021) have been detected and *PcP*, $P_{\mathrm{diff}}$ and $S_{\mathrm{diff}}$ could potentially be detected in future work. These corrections are for a station fixed at the InSight lander location (4.50°N, 135.62°E) and with source depths between 0 and 50 km, as this is the range of source depths used in previous studies (e.g. Khan *et al.* 2021; Stähler *et al.* 2021). These corrections cover a full range of back-azimuths and distances; however, a large proportion of the events on the Mars that have so far been located have been in the Cerberus Fossae region (e.g. Khan *et al.* 2021). Ellipticity corrections and arrival times for an event located at the centre of the Cerberus Fossae region (11.28°N, 166.37°E) to the InSight lander are shown in Table 1. The magnitude of these corrections is negligible compared to the magnitude on the uncertainty of the phase picks by the Marsquake Service (MQS) which can be up to 60 s (Clinton *et al.* 2021). Furthermore, due to the uncertainty of the source location, Martian studies to date have relied on differential times (e.g. Drilleau *et al.* 2021; Durán *et al.* 2022) for which ellipticity corrections are expected to be even less significant.

## 5 CONCLUSIONS

We have produced a Python package, EllipticiPy, which allows the easy calculation of ellipticity corrections that is designed to work alongside ObsPy TauP. This package is versatile and can calculate an ellipticity correction for any ray path that ObsPy TauP can return and removes the reliance on inaccurate and incomplete tables of ellipticity coefficients.

On the Earth, ellipticity corrections are of the order of single seconds and should therefore be routinely applied when working with higher frequency seismic observations where trends on this order are to be interpreted. On the Mars, ellipticity corrections are of approximately the same magnitude as on the Earth, but are far smaller than the magnitude of the uncertainty on the phase picks given by the Marsquake Service. At present, ellipticity corrections on the Mars are therefore negligible but this may not be the case in the future.

## ACKNOWLEDGMENTS

For the purpose of open access, the author has applied a Creative Commons Attribution (CC BY) licence to any author accepted manuscript version arising from this submission. This project has received funding from the European Research Council (ERC) under the European Union's Horizon 2020 - Research and Innovation Framework Programme (grant agreement No. 804071 -ZoomDeep). JCEI acknowledges support from UKSA grant ST/W002515/1. The synthetic modelling in this work was performed using resources provided by the Cambridge Service for Data Driven Discovery (CSD3) operated by the University of Cambridge Research Computing Service (www.csd3.cam.ac.uk), provided by Dell EMC and Intel using Tier-2 funding from the Engineering and Physical Sciences Research Council (capital grant EP/T022159/1), and DiRAC funding from the Science and Technology Facilities Council (www.dirac.ac.uk).

The authors would like to thank past and present members of the University of Cambridge Global Seismology research group, especially Carl Martin, George Pindar, Alistair Boyce and Florian Millet for helpful and insightful scientific discussions. The authors would also like to thank Brian Kennett and Olafur Gudmundsson for their personal communications regarding their previous works. The authors would also like to thank the editor, Carl Tape, as well as Istvan Bondar and one anonymous reviewer for their constructive comments and helping to improve the original manuscript.

## DATA AVAILABILITY

Data analysis and production of figures was performed using Python, especially ObsPy (Beyreuther *et al.* 2010). The routines of Kennett & Gudmundsson (1996) can be found at: https://github.com/GeoscienceAustralia/ellip-corr in a convenient format within a Python wrapper. The coefficients of Kennett & Gudmundsson (1996) can also be found in PDF format: http://rses.anu.edu.au/seismology/AK135tables.pdf.

For EllipticiPy, the source code, installation instructions, example usage and tables of coefficients can be found at this project's GitHub page: https://github.com/StuartJRussell/EllipticiPy.

## REFERENCES

Beyreuther, M., Barsch, R., Krischer, L., Megies, T., Behr, Y. & Wassermann, J., 2010. ObsPy: a Python toolbox for seismology, *Seismol. Res. Lett.,* **81**(3), 530–533.

Bills, B. G. & Ferrari, A. J., 1978. Mars topography harmonics and geophysical implications, *J. geophys. Res.,* **83**(B7), 3497–3508.

Buland, R. & Chapman, C., 1983. The computation of seismic travel times, *Bull. seism. Soc. Am.,* **73**(5), 1271–1302.

Bullen, K., 1937. The ellipticity correction to travel times of *P* and *S* earthquake waves, *Mon. Not. Roy. Astron. Soc., Geophys. Suppl.,* **4**(2), 143–157.

Bullen, K. E. & Bolt , B. A.,1985. *An Introduction to the Theory of Seismology,* Cambridge Univ. Press.

Bullen, K. E., 1975. *The Earth's Density,* Chapman and Hall, London.

Clinton, J. F. *et al.*, 2021. The Marsquake catalogue from InSight, sols 0–478, *Phys. Earth planet. Inter.,* **310,** 106595.

Crotwell, P., Owens, T. & Ritsema, J., 1999. The TauP toolkit: flexible seismic travel-time and ray-path utilities, *Seismol. Res. Lett.,* **70**(2), 154–160.

Doornbos, D. J., 1988. Asphericity and ellipticity corrections, in *Seismological Algorithms,* pp. 75–85, ed. Doornbos, D. J., Academic Press.

Drilleau, M., Samuel, H., Rivoldini, A., Panning, M. & Lognonné, P., 2021. Bayesian inversion of the Martian structure using geodynamic constraints, *Geophys. J. Int.,* **226**(3), 1615–1644.

Durán, C., Khan, A., Ceylan, S., Zenhäusern, G., Stähler, S., Clinton, J. & Giardini, D., 2022. Seismology on Mars: an analysis of direct, reflected, and converted seismic body waves with implications for interior structure, *Phys. Earth planet. Inter.,* **325,** 106851.

Dziewonski, A. & Gilbert, F., 1976. The effect of small, aspherical perturbations on travel times and a re-examination of the corrections for ellipticity, *Geophys. J. R. astr. Soc.,* **44,** 7–17.

Dziewonski, A., Hales, A. & Lapwood, E., 1975. Parametrically simple Earth models consistent with geophysical data, *Phys. Earth planet. Inter.,* **10,** 12–48.

Dziewonski, A. M. & Anderson, D., 1981. Preliminary Reference Earth Model, *Phys. Earth planet. Inter.,* **25**(4), 297–356.

Garcia, R. F. *et al.*, 2019. Lunar seismology: an update on interior structure models, *Space Sci. Rev.,* **215**(8), 1–47.

Jeffreys, H., 1935. On the ellipticity correction in seismology, *Geophys. J. Int.,* **3,** 271–274.

Kennett, B. & Gudmundsson, O., 1996. Ellipticity corrections for seismic phases, *Geophys. J. Int.,* **127**(1), 40–48.

Kennett, B., Engdahl, E. & Buland, R., 1995. Constraints on seismic velocities in the Earth from traveltimes, *Geophys. J. Int.,* **122**(1), 108–124.

Khan, A. *et al.*, 2021. Upper mantle structure of Mars from InSight seismic data, *Science,* **373**(6553), 434–438.

Knapmeyer-Endrun, B. *et al.*, 2021. Thickness and structure of the martian crust from InSight seismic data, *Science,* **373**(6553), 438–443.

Komatitsch, D. & Tromp, J., 2002a. Spectral-element simulations of global seismic wave propagation-I. Validation, *Geophys. J. Int.,* **149**(2), 390–412.

Komatitsch, D. & Tromp, J., 2002b. Spectral-element simulations of global seismic wave propagation—II. Three-dimensional models, oceans, rotation and self-gravitation, *Geophys. J. Int.,* **150**(1), 303–318.

Latham, G. *et al.*, 1973. Lunar structure and dynamics-results from the Apollo passive seismic experiment, *Moon,* **7**(3), 396–421.

Stähler, S. C. *et al.*, 2021. Seismic detection of the martian core, *Science,* **373**(6553), 443–448.

Tanaka, S., 2007. Possibility of a low *P*-wave velocity layer in the outermost core from global *SmKS* waveforms, *Earth planet. Sci. Lett.,* **259**(3–4), 486–499.

Tanaka, S., 2010. Constraints on the core–mantle boundary topography from *P4KP-PcP* differential travel times, *J. geophys. Res.,* **115,** B04310.

Tian, Y., Hung, S.-H., Nolet, G., Montelli, R. & Dahlen, F. A., 2007. Dynamic ray tracing and traveltime corrections for global seismic tomography, *J. Comput. Phys.,* **226**(1), 672–687.

Wu, W. & Irving, J. C. E., 2020. Array-based iterative measurements of travel times and their constraints on outermost core structure, *J. geophys. Res.,* **125**(3), e2019JB018162.

## SUPPORTING INFORMATION

Supplementary data are available at *GJI* online.

**Table S1**. Minimum and maximum ellipticity corrections for commonly used seismic phases in PREM. Corrections for depth phases can be calculated but are not shown here.

Please note: Oxford University Press is not responsible for the content or functionality of any supporting materials supplied by the authors. Any queries (other than missing material) should be directed to the corresponding author for the paper.